SECURITY INFORMATION

244

Copy
RM E53G10

[redacted]

NACA RM E53G10

TECH LIBRARY KAFB, NM
0143387

6830

NACA

RESEARCH MEMORANDUM

INVESTIGATION OF TRANSLATING-SPIKE SUPERSONIC INLET AS MEANS OF MASS-FLOW CONTROL AT MACH NUMBERS OF 1.5, 1.8, AND 2.0

By Gerald C. Gorton

Lewis Flight Propulsion Laboratory
Cleveland, Ohio

[redacted]

NATIONAL ADVISORY COMMITTEE
FOR AERONAUTICS
WASHINGTON
October 29, 1953

[redacted]

TECH LIBRARY KAFB, NM
0143387

 [redacted]

NATIONAL ADVISORY COMMITTEE FOR AERONAUTICS

RESEARCH MEMORANDUM

INVESTIGATION OF TRANSLATING-SPIKE SUPERSONIC INLET AS MEANS OF MASS-FLOW CONTROL AT MACH NUMBERS OF 1.5, 1.8, and 2.0

By Gerald C. Gorton

2948

CC-1

SUMMARY

In order to check the practicability of a translating-spike inlet, an investigation was conducted in the 8- by 6-foot supersonic wind tunnel on a 50° conical-spike inlet at Mach numbers of 1.5, 1.8, and 2.0 over a range of angle of attack from 0° to 9°.

The additive-drag penalty associated with inlet mass-flow spillage was significantly reduced by using a translating-spike inlet rather than a fixed-geometry inlet. However, the total-pressure recovery of this translating-spike inlet with oblique shock spillage was less than the total-pressure recovery of the fixed-geometry inlet at the same mass-flow spillage.

Indications of the improvement in performance of a turbojet installation by means of mass-flow control with this specific variable-geometry inlet are included.

INTRODUCTION

When turbojet engines are operated over a range of altitudes, engine speeds, and flight Mach numbers, some form of variable-inlet geometry is needed to efficiently match the mass-flow requirements of the engine to the air delivered by the inlet. One proposed matching method prescribes the use of an inlet with a translating spike which would allow the required amount of mass flow to be spilled with a minimum of additive drag. Additional means of mass-flow control are discussed in references 1 and 2.

A preliminary investigation (ref. 3) of a translating-spike inlet has been made, but the available information is limited to internal flow performance at zero angle of attack. The object of the present

[redacted]

[redacted]

investigation was to ascertain the practicability of a translating-spike inlet as a means of mass-flow control and to obtain total-pressure-recovery data at angle of attack and drag data at zero angle of attack. The over-all gain in performance of an engine equipped with a translating-spike inlet is determined by the combination of changes in total-pressure recovery and drag relative to the values obtainable with a fixed-spike inlet. This investigation was conducted at the NACA Lewis laboratory.

2948

SYMBOLS

The following symbols are used in this report:

A	flow area, sq ft
A_i	inlet capture area defined by cowl lip, sq ft
A_m	maximum external cross-sectional area, sq ft
C_D	external-drag coefficient, D/q_0A_m
$C_{D,a}$	additive-drag coefficient, D_a/q_0A_i
D	drag force, lb
D_a	additive-drag force, lb
D_s	drag force due to mass-flow spillage, lb
F_n	thrust at operating total-pressure recovery, lb
$F_{n,i}$	thrust at 100 percent total-pressure recovery, lb
L	length of model, excluding conical-spike projection, in.
M	Mach number
m	mass flow, slugs/sec
m_0	mass flow through stream tube defined by cowl lip, slugs/sec
P	total pressure, lb/sq ft
p	static pressure, lb/sq ft
q	dynamic pressure, $\gamma pM^2/2$, lb/sq ft

x axial distance downstream of cowl lip, in.

α angle of attack, deg

γ ratio of specific heats for air

θ_l cowl-position parameter (angle between axis of diffuser and line joining apex of cone to cowl lip), deg

φ theoretical oblique shock angle, deg

Subscripts:

0 free stream

3 plane of survey

4 diffuser outlet station, sting in

4,1 diffuser outlet station, sting out

x axial station

APPARATUS AND PROCEDURE

The sting-mounted 8-inch-diameter model was installed in the 8- by 6-foot supersonic wind tunnel which was operated at Mach numbers M_0 of 1.5, 1.8, and 2.0. The Reynolds number during the investigation was approximately 3.4×10^6, based on the maximum external diameter of the model (8.125 in.).

The model was investigated with three inlets, one of which was on-design at a free-stream Mach number M_0 of 1.5, one at 1.8, and one at 2.0. These inlets were designed such that the cone shoulders of their respective 50° conical spikes were positioned at the cowl-lip station. The cone shoulder is that portion of the spike where the contour deviates from a straight conical taper. The inlets designed for $M_0 = 1.5$ and 1.8 were investigated at zero angle of attack. The inlet designed for $M_0 = 2.0$ was used in conjunction with faired spacers to obtain spike translation and was investigated at angles of attack from 0° to 9°. The spacers made possible the positioning of the conical spike at cowl-position parameters θ_l of 54.1°, 45.8°, 43.0°, 39.3°, 36.5°, and 34.1°. The first three values of θ_l allow the oblique shock generated by the cone to fall at the cowl lip at $M_0 = 1.5$, 1.8, and 2.0, respectively.

2948

CC-1 back

[redacted]

At $M_0 = 2.0$, the last three values of θ_l cause 9, 19.5, and 27.5 percent mass-flow spillage, respectively. Hereinafter, these spacer configurations will be referred to as the translating-spike inlet.

The principal dimensions and notation for the various configurations are presented in table I, and the coordinates of the cowls, conical spikes, and faired spacers are given in tables II and III. A schematic diagram of the model including details of the faired-spacer assembly is given in figure 1. The diffuser area-variation curves are presented in figure 2 along with a schematic diagram of the model on which the pertinent stations are indicated. 2948

The instrumentation consisted of a static-pressure rake at the plane of survey (station 3), a three-component strain-gage balance within the model centerbody, a movable plug at the outlet of the model to control the mass flow, a direct-reading angle-of-attack indicator, and a dynamic-pressure pickup located slightly downstream from the plane of survey. The dynamic-pressure pickup was used in conjunction with schlieren apparatus to determine inlet-flow instability.

The Mach number at the plane of survey was determined from an isentropic one-dimensional area-ratio existing between the plane of survey and the choked outlet. The diffuser outlet Mach number $M_{4,1}$ is defined as that Mach number calculated by isentropically expanding the flow to the internal-duct area, at station 4 with the sting removed.

The mass-flow ratio presented is the ratio of mass flow through the model m_3 to that of a free-stream tube defined by the capture area of the inlet cowl. The mass flow at the plane of survey was calculated by assuming a choked condition at the outlet-nozzle throat and using the measured average static pressure and the calculated diffuser Mach number at the plane of survey. An outlet-nozzle flow coefficient of 0.98 was used.

Total-pressure recovery is the ratio of the total pressure P_3, determined from the measured average static pressure and the calculated Mach number at the plane of survey, to the measured free-stream total pressure, P_0.

Drag data were computed from axial-force readings of the three-component strain-gage balance.

DISCUSSION OF RESULTS

Effect of spike translation at zero angle of attack. - Total-pressure recovery, diffuser outlet Mach number, and external drag

coefficient are presented in figure 3 as a function of mass-flow ratio for the translating-spike inlet at zero angle of attack. These performance characteristics at critical operation are summarized in figure 4 as a function of the cowl-position parameter θ_l. Additional data, not presented in figure 3 are also used in making the summary plots of figure 4.

The total-pressure recovery is maximum for $M_0 = 1.8$ and 2.0 at $\theta_l = 43.0^\circ$ and decreases as the spike is translated to either higher or lower values of θ_l. The drop in total-pressure recovery for $\theta_l < 43.0^\circ$ arises from the flow expansion over the cone shoulder upstream of the cowl lip. (See fig. 5(d), for example.) The decrease in total-pressure recovery for $\theta_l > 43.0^\circ$ is a result of the normal shock being forced outside the cowl lip because of excessive internal contraction (see fig. 5(e)) and the fact that the oblique shock moves downstream as θ_l increases. Both conditions increase the amount of mass flow passing through a normal shock at free stream Mach numbers.

2948

At $M_0 = 1.5$, the inlet appears to be less susceptible to losses in total pressure associated with the expanded-flow region over the shoulder. However, the inlet does suffer a drop in total-pressure recovery for $\theta_l > 45.8^\circ$ because of excessive internal contraction (see fig. 5(i)).

The variation of diffuser outlet Mach number with spike translation at zero angle of attack, as shown in figure 4, results from changes in total-pressure recovery and mass-flow ratio at critical operation of the translating-spike inlet.

Variation of the total drag with θ_l is most pronounced at $M_0 = 1.8$ and 2.0 with the minimum values occurring where θ_l equals the theoretical oblique shock angle φ. The increase in total drag for $\theta_l < \varphi$ is the result of the additive drag associated with mass-flow spillage downstream of an oblique shock, whereas the increase in total drag for $\theta_l > \varphi$ is due to spillage downstream of a normal shock. This spillage downstream of the normal shock results from inability of the inlet to swallow the normal shock because of internal contraction. The total drag at $M_0 = 1.5$ is essentially constant over the range of θ_l, with the effects of internal contraction most noticeable at $\theta_l = \varphi$.

Analysis indicates that an inlet can be designed which will keep the cone shoulder downstream of the cowl lip for the entire range of spike translation, without internal contraction. It is expected that such a design would retain the higher critical total-pressure recovery of the fixed-spike inlet throughout the range of translation.

However, the redesigned inlet requires the internal cowl-lip angle to be increased from 7° to 18°, thereby increasing the cowl pressure-drag coefficient from approximately 0.035 to 0.056 based on the maximum external cross-sectional area as determined from linearized potential theory.

Effect of spike translation at angle of attack. - The total-pressure recovery characteristics with the spike adjusted for $\theta_l = \varphi$ and also extended to $\theta_l = 39.3°$, 36.5°, and 34.1° (corresponding to 9, 19.5, and 27.5 percent spillage at $M_0 = 2.0$) are presented in figure 6 as a function of mass-flow ratio for the various angles of attack investigated. The critical total-pressure recovery and mass-flow ratios for the translating-spike inlet are summarized in figure 7 as a function of angle of attack. 2948

The total-pressure recovery and mass-flow ratios at critical operation decrease with increased angle of attack for the various spike positions, and, in general, the same trend in critical total-pressure recovery and mass-flow ratio with spike projection is obtained at angles of attack as was previously indicated, figure 4, for zero angle of attack.

Performance comparison of translating-spike inlet with fixed-spike inlet. - The total-pressure recovery and drag of the translating-spike inlet at critical operation is compared (fig. 8) to the subcritical operation of the fixed-spike inlet, 2.0-43.0, for the range of Mach numbers investigated and zero angle of attack. This particular fixed-spike inlet was selected for the comparison because it is a high-performance inlet at $M_0 = 1.5$ and 1.8 as well as the on-design Mach number, 2.0.

As shown in figure 8, total-drag was reduced by obtaining spillage with a translating-spike inlet at critical operation. This reduction results from the lower additive drag associated with oblique shock mass-flow spillage as compared to the inlet normal shock mass-flow spillage of a fixed-spike inlet forced to operate subcritically to match the engine requirements.

The total-pressure recovery of the translating-spike inlet with supersonic spillage is lower than the total-pressure recovery of the fixed-spike inlet, for the same amount of mass-flow spillage, throughout the range of Mach numbers investigated. However, this may be characteristic of only the particular design compromise selected for these inlets.

The propulsive thrust of a turbojet engine equipped with the translating-spike inlet would tend to be increased, relative to that

of a fixed-spike inlet, as a result of the decreased spillage drag, but tend to be decreased as a result of the lower total-pressure recovery. Any change in over-all performance is the combined effect of drag and total-pressure recovery. An example of this may be seen in reference 4, where a comparison was made by sizing both the fixed-spike inlet and the translating-spike inlet to a turbojet engine at $M_0 = 0.85$ and operating at $M_0 = 1.5$, 1.8, and 2.0. This engine exhibited a gain in effective thrust $\frac{F_n - D_s}{F_{n,i}}$ of 2.5 percent at $M_0 = 1.5$, 6.5 percent at $M_0 = 1.8$, and 2.5 percent at $M_0 = 2.0$ when the translating-spike inlet was used.

2940

Comparison of experimental additive drag with theoretical predictions. - The aforementioned analysis indicated that any gain in turbojet engine performance, when a translating-spike inlet is used to obtain the mass-flow spillage necessary for engine-inlet matching, most probably will result from reductions in the additive drag of the inlet. A theoretical means of predicting additive drag (ref. 5) is compared with the experimental values of this investigation.

Theoretical inlet normal shock additive drag is compared in figure 9 with the experimental values for inlets 2.0-43.0, 1.8-46.9, and 1.5-54.5 at their respective design Mach numbers. The experimental inlet normal shock additive drag is defined as the difference between the spillage drag and the change in cowl-pressure and friction drag as the inlet goes subcritical. The spillage drag is the total drag at a given mass-flow ratio minus the total drag with zero spillage. Configurations 1.8-46.9 and 1.5-54.5 experienced critical mass-flow spillage, and the drag curves were extrapolated to unity mass-flow ratio. Data for a similar configuration (ref. 6) were used to estimate the change in cowl-pressure and friction drag with decreasing mass-flow ratio at $M_0 = 1.8$ and 2.0.

The theoretical curves for inlet normal shock additive drag were calculated from equation (8) of reference 5 by use of the assumptions that the subcritical total-pressure recovery and the static pressure along the cone surface remained constant. The correlation between the theoretical and the experimental additive drag at $M_0 = 1.8$ and 2.0 is excellent. Experimental cowl-pressure-drag data were not available to make the correlation at $M_0 = 1.5$.

Also indicated in figure 9 is a comparison of the experimental oblique shock spillage drag and theoretical oblique shock additive drag of the translating-spike inlet. The experimental oblique shock spillage drag is defined as the total drag at critical operation for a given spike projection minus the total drag at critical operation with the spike positioned for zero spillage. The internal contraction with configurations 2.0-45.8 and 2.0-54.1 caused the normal shock to position

itself upstream of the cowl lip (see figs. 5(e) and 5(i)) and made it necessary to extrapolate the total-drag curve to unity mass-flow ratio.

The theoretical curves taken from figure 7, reference 5, show reasonable correlation with the experimental data, with the best agreement at the higher Mach numbers and the higher mass-flow ratios. It is doubtful if better correlation could be expected, since the theory is based on a conical flow field at the cowl lip, whereas the experimental values are from configurations with an expanded flow field over the cone shoulder and upstream of the cowl lip.

2948

SUMMARY OF RESULTS

The following results were obtained in an investigation of a specific translating-spike inlet used as a means of mass-flow control over a range of free-stream Mach numbers from 1.5 to 2.0 and at angles of attack from 0° to 9°.

1. The drag penalty associated with inlet mass-flow spillage was significantly reduced by using a translating-spike inlet rather than a fixed-geometry inlet. However, for the particular design investigated, the gain in engine performance resulting from reduced additive drag was partially nullified by a decrease in the critical total-pressure recovery of the translating-spike inlet relative to the subcritical total-pressure recovery of the fixed-geometry inlet for the same amount of mass-flow spillage.

2. The translating-spike inlet experienced a decrease in the critical total-pressure recovery and mass-flow ratio with increasing angle of attack for any one spike position, similar to a fixed-spike inlet on-design. Also, at a given angle of attack, the effect of spike translation on critical total-pressure recovery and mass-flow ratio was, in general, similar to that of the zero angle-of-attack performance.

Lewis Flight Propulsion Laboratory
National Advisory Committee for Aeronautics
Cleveland, Ohio, July 20, 1953

REFERENCES

1. Hayes, Clyde: Preliminary Investigation of a Variable Mass-Flow Supersonic Nose Inlet. NACA RM L9J11, 1949.

2. Allen, J. L., and Beke, Andrew: Force and Pressure Recovery Characteristics at Supersonic Speeds of a Conical Spike Inlet with Bypasses Discharging in an Axial Direction. NACA RM E52K14, 1953.

[redacted]

3. Hinners, Arthur H., Jr., and Lee, John B.: Preliminary Investigation of the Total-Pressure-Recovery Characteristics of a 15° Semiangle Movable-Cone Variable-Geometry Ram-Jet Inlet at Free-Jet Mach Numbers of 1.62, 2.00, 2.53, and 3.05. NACA RM L52K10, 1953.

4. Allen, J. L., and Beke, Andrew: Performance Comparison at Supersonic Speeds of Inlets Spilling Excess Flow by Means of Bow Shock, Conical Shock, or Bypass. NACA RM E53H11, 1953.

5. Sibulkin, Merwin: Theoretical and Experimental Investigation of Additive Drag. NACA RM E51B13, 1951.

6. Weinstein, Maynard I., and Davids, Joseph: Force and Pressure Characteristics for a Series of Nose Inlets at Mach Numbers from 1.59 to 1.99. III - Conical-Spike All-External-Compression Inlet with Supersonic Lip. NACA RM E50J30, 1951.

2948

CC-2

[redacted]

TABLE I. - PRINCIPAL DIMENSIONS AND NOTATIONS FOR

CONFIGURATIONS INVESTIGATED

[Maximum external cross-sectional area, 0.360 sq ft; maximum diffuser flow area, 0.289 sq ft; over-all length, 55.875 in.; lip radius, 0.005 in.; internal lip angle, 7°.]

2948

Inlet configuration (a)	Inlet capture area, sq ft	External lip angle, deg
2-54.1	0.1545	12
2-45.8	.1545	12
2-43.0	.1545	12
2-39.3	.1545	12
2-36.5	.1545	12
2-34.1	.1545	12
1.8-46.9	.1422	11
1.5-54.5	.1290	11

NACA

[a]First number refers to design free-stream Mach number, second number to cowl-position parameter.

2948

CC-2 back

TABLE II. - COORDINATES FOR COWLS AND CONICAL SPIKES FOR CONFIGURATIONS INVESTIGATED

[All dimensions given in inches.]

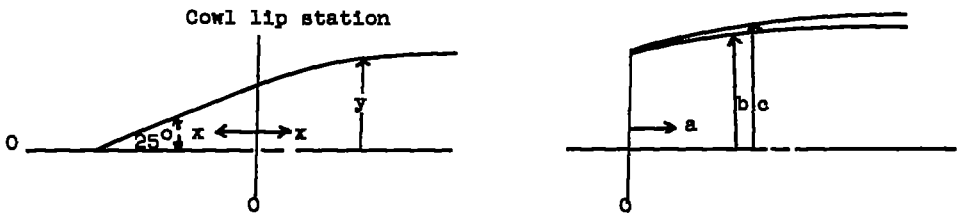

1.5-54.5 Inlet designed for oblique shock to fall at cowl lip at $M_0 = 1.5$ with cone shoulder at cowl-lip station.

1.8-46.9 Inlet designed for oblique shock to fall at cowl lip at $M_0 = 1.8$ with cone shoulder at cowl-lip station.

2.0-43.0 Inlet designed for oblique shock to fall at cowl lip at $M_0 = 2.0$ with cone shoulder at cowl-lip station.

(a) 1.5-54.5

x	y	a	b	c
-1.70	Conical	0	2.43	2.43
0	0.80	1.0	Conical	2.82
.10	.84	1.25		2.67
.20	.88	1.50		2.72
.30	.91	1.75		2.75
.50	.97	2.00		2.79
1.00	1.11	Conical		Conical
1.50	1.24			
2.00	1.36			
2.50	1.48	6.80	3.25	3.38
3.00	1.59	7.00	3.28	3.40
3.50	1.69	7.20	3.29	3.42
4.00	1.79	7.40	3.31	3.43
4.50	1.89	7.60	3.32	3.44
5.00	1.98	7.80	3.33	3.45
5.50	2.07	Conical	Conical	Conical
6.00	2.16			
6.36	2.22			
		8.67	3.35	3.47

(b) 1.8-46.9

x	y	a	b	c
-2.41	Conical	0	2.55	2.55
0	1.12	4.60	3.12	3.24
.1	1.16	5.60	3.22	3.34
.25	1.21	7.60	3.29	3.41
.40	1.26	8.60	3.32	3.44
1.10	1.42	8.67	3.35	3.47
2.10	1.64			
3.10	1.84			
4.10	2.03			
5.18	2.21			

(c) 2.0-43.0

x	y	a	b	c
-2.86	0	Conical	2.66	2.66
0	1.32	.25	2.69	2.74
.2	1.39	.50	2.73	2.79
.4	1.45	1.00	2.80	2.89
.6	1.51	2.00	2.93	3.04
1.0	1.61	3.00	3.04	3.16
2.0	1.84	4.00	3.13	3.25
3.0	2.01	5.00	3.20	3.32
4.0	2.14	6.00	3.25	3.38
4.94	2.24	7.00	3.30	3.42
		8.00	3.33	3.45
		8.67	3.35	3.47

[redacted]

2948

TABLE III. - FAIRED SPACERS USED TO SIMULATE TRANSLATING-SPIKE INLET

[All dimensions given in inches.]

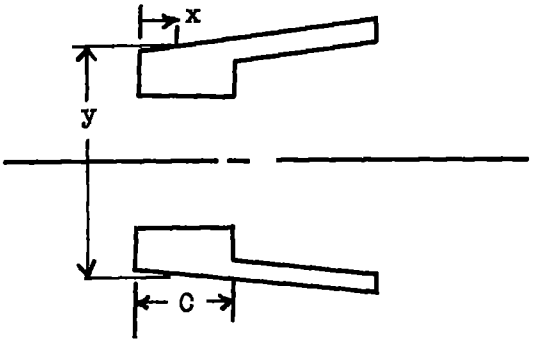

Configuration	C
2.0-54.1	0.43
2.0-45.8	1.08
2.0-43.0	1.36
2.0-39.3	1.76
2.0-36.5	2.12
2.0-34.1	2.44

2.0-54.1		2.0-45.8		2.0-43.0	
x	y	x	y	x	y
0	4.47	0	4.47	0	4.47
.50	4.55	.50	4.55	.50	4.55
1.00	4.61	1.00	4.61	1.00	4.61
1.25	4.69	1.50	4.70	1.50	4.68
1.50	4.76	2.00	4.76	2.0	4.73
1.79	4.80	2.44	4.80	2.5	4.78
				2.72	4.80

2.0-39.3		2.0-36.5		2.0-34.1	
x	y	x	y	x	y
0	4.47	0	4.47	0	4.47
.50	4.55	.50	4.55	.50	4.55
1.00	4.61	1.00	4.61	1.00	4.61
1.50	4.67	1.50	4.67	1.50	4.67
2.00	4.73	2.00	4.71	2.00	4.71
2.50	4.74	2.50	4.74	2.50	4.74
3.12	4.80	3.00	4.77	3.00	4.76
		3.48	4.80	3.50	4.79
				3.80	4.80

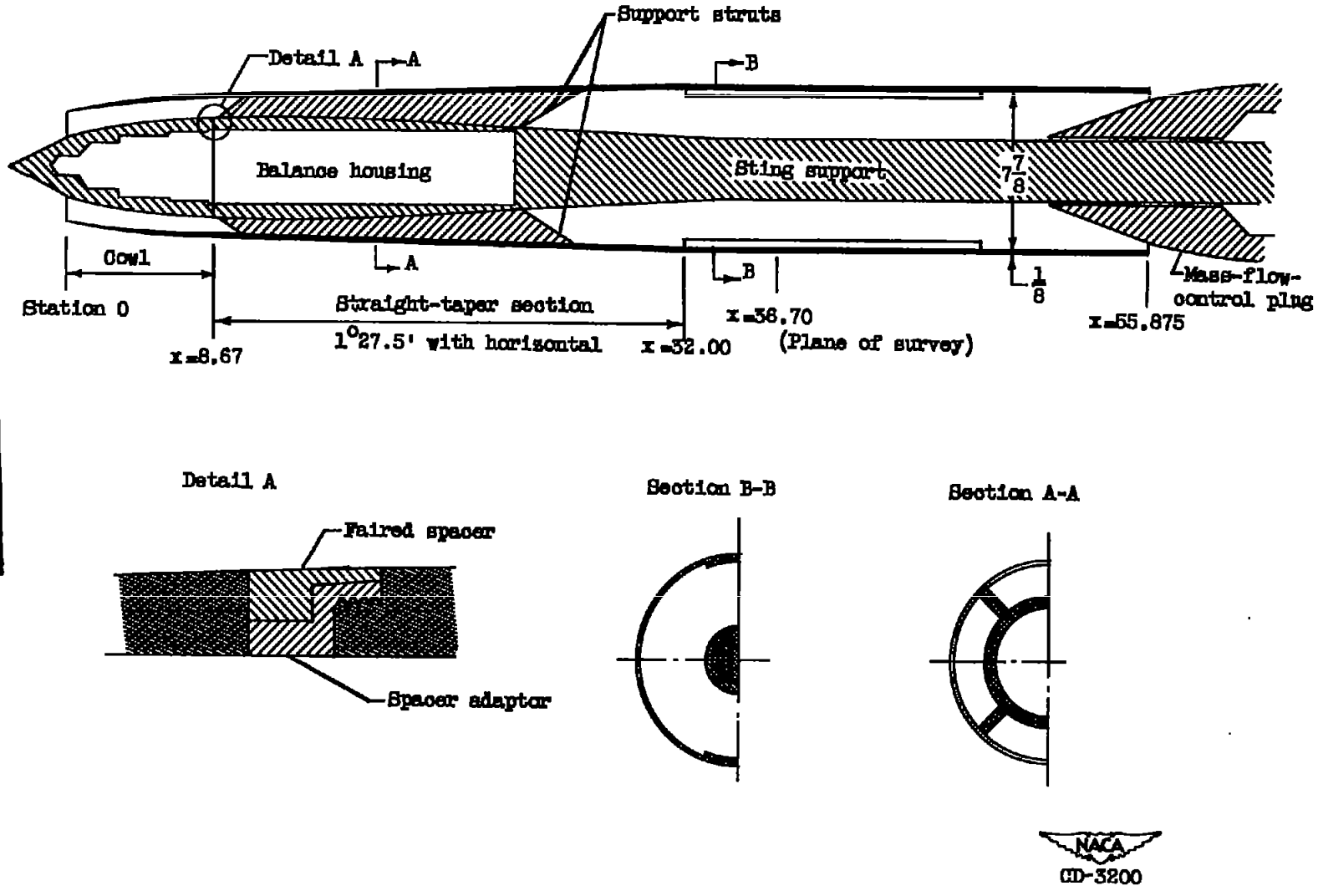

Figure 1. - Schematic diagram of 8-inch-diameter model and details of faired-spacer assembly.

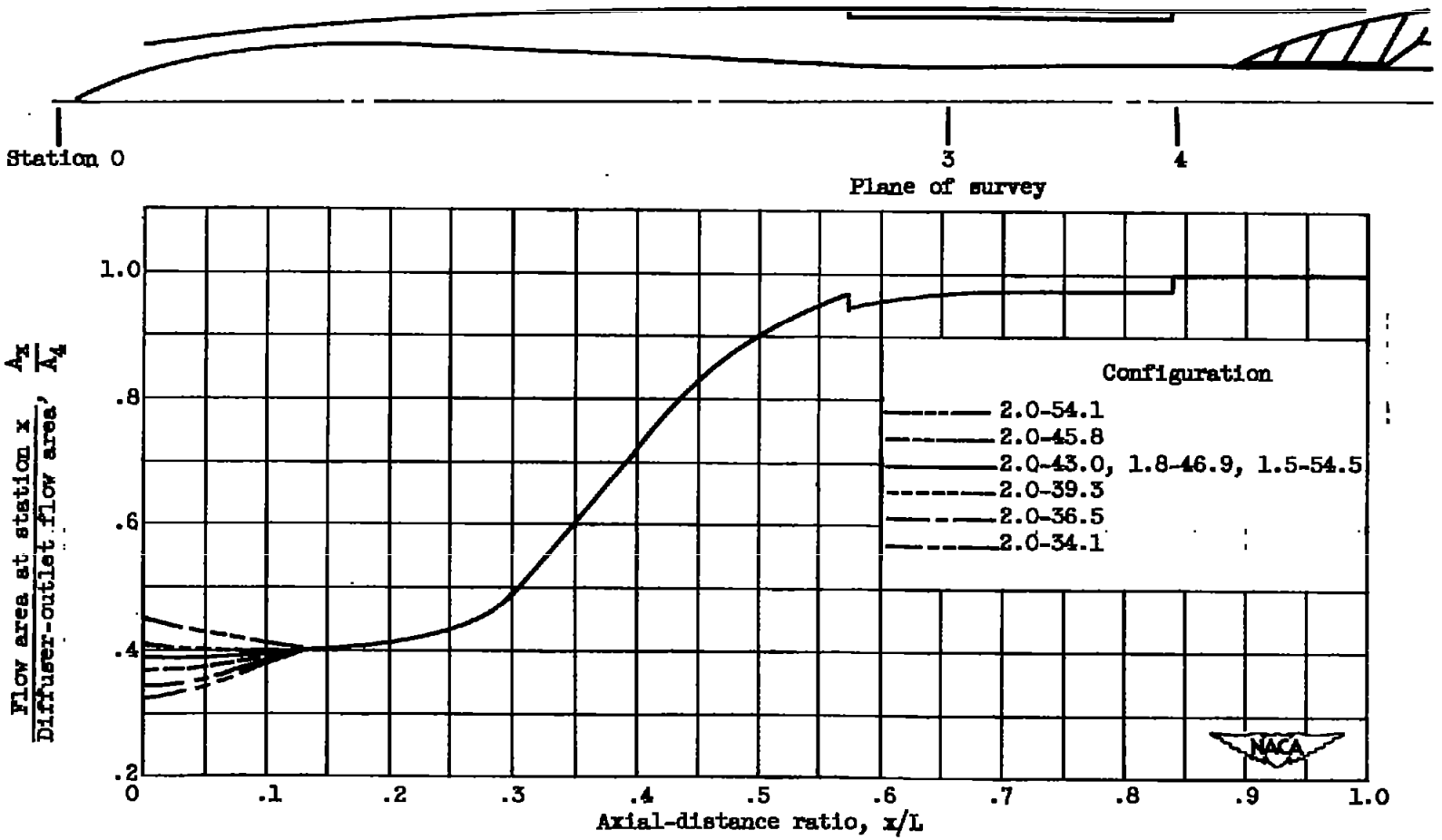

Figure 2. - Diffuser flow-area variation.

2948

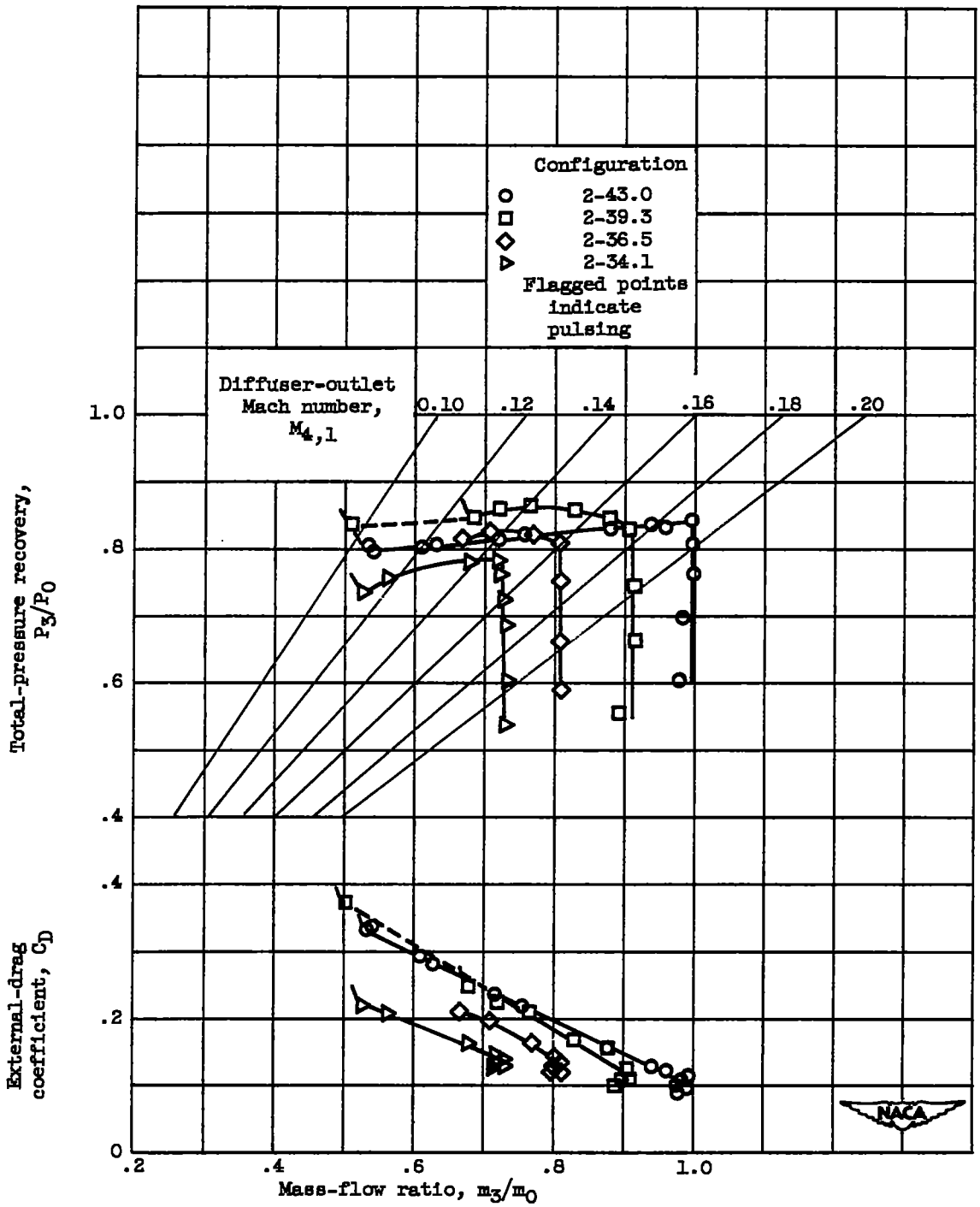

(a) Free-stream Mach number, 2.0.

Figure 3. - Performance of translating-spike inlet at zero angle of attack for various values of cowl-position parameter.

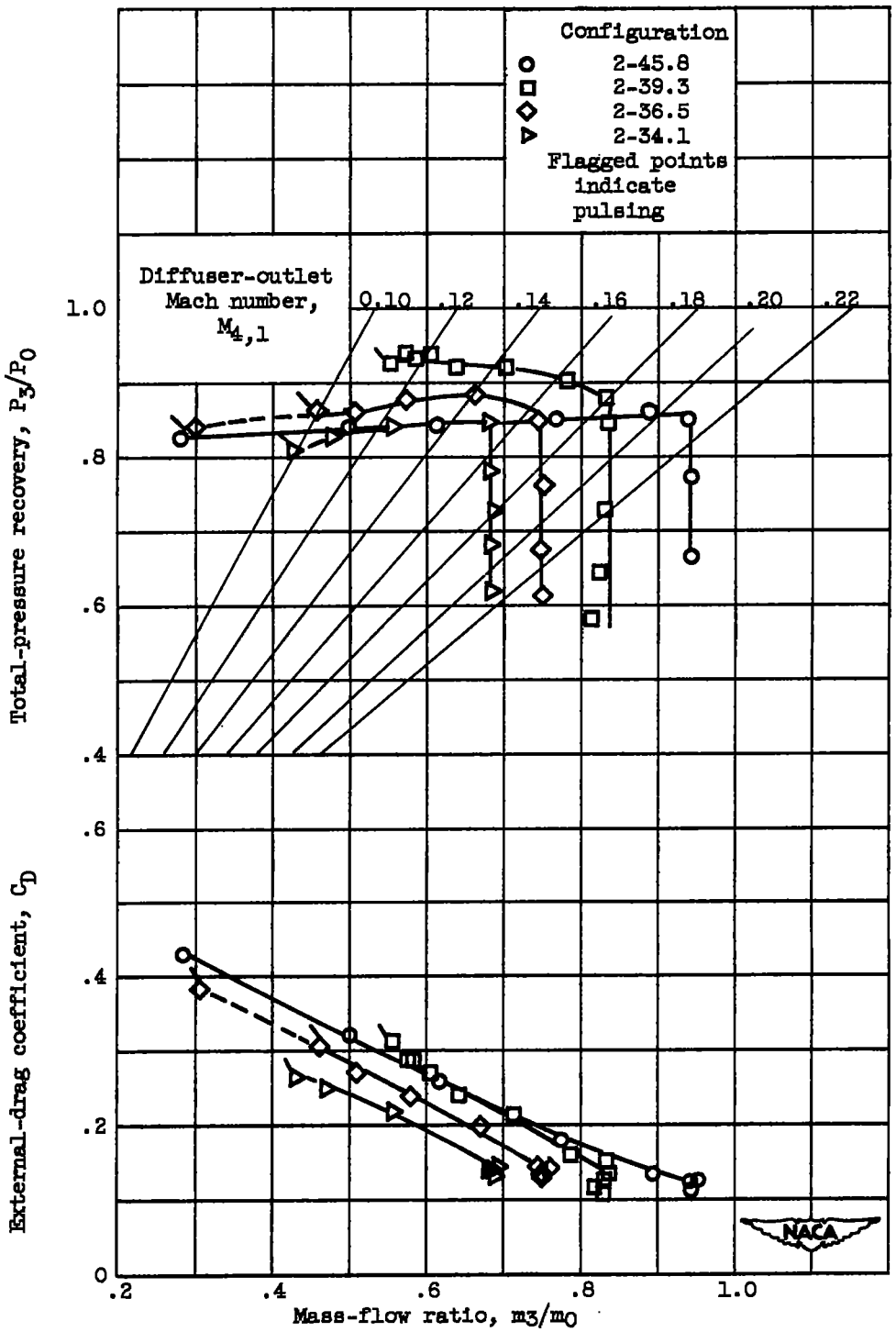

(b) Free-stream Mach number, 1.8.

Figure 3. - Continued. Performance of translating-spike inlet at zero angle of attack for various values of cowl-position parameter.

2948

CC-3

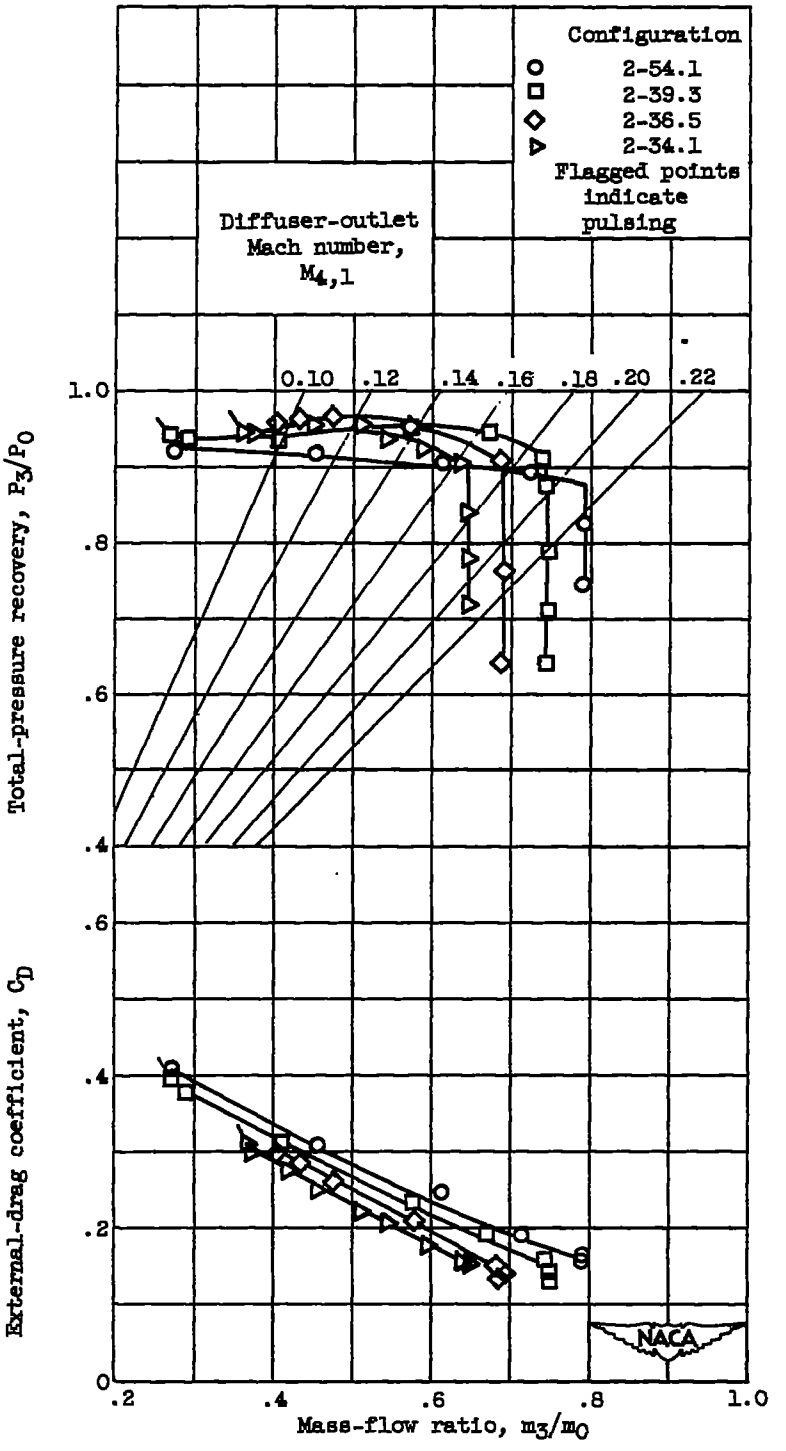

(c) Free-stream Mach number, 1.5.

Figure 3. - Concluded. Performance of translating-spike inlet at zero angle of attack for various values of cowl-position parameter.

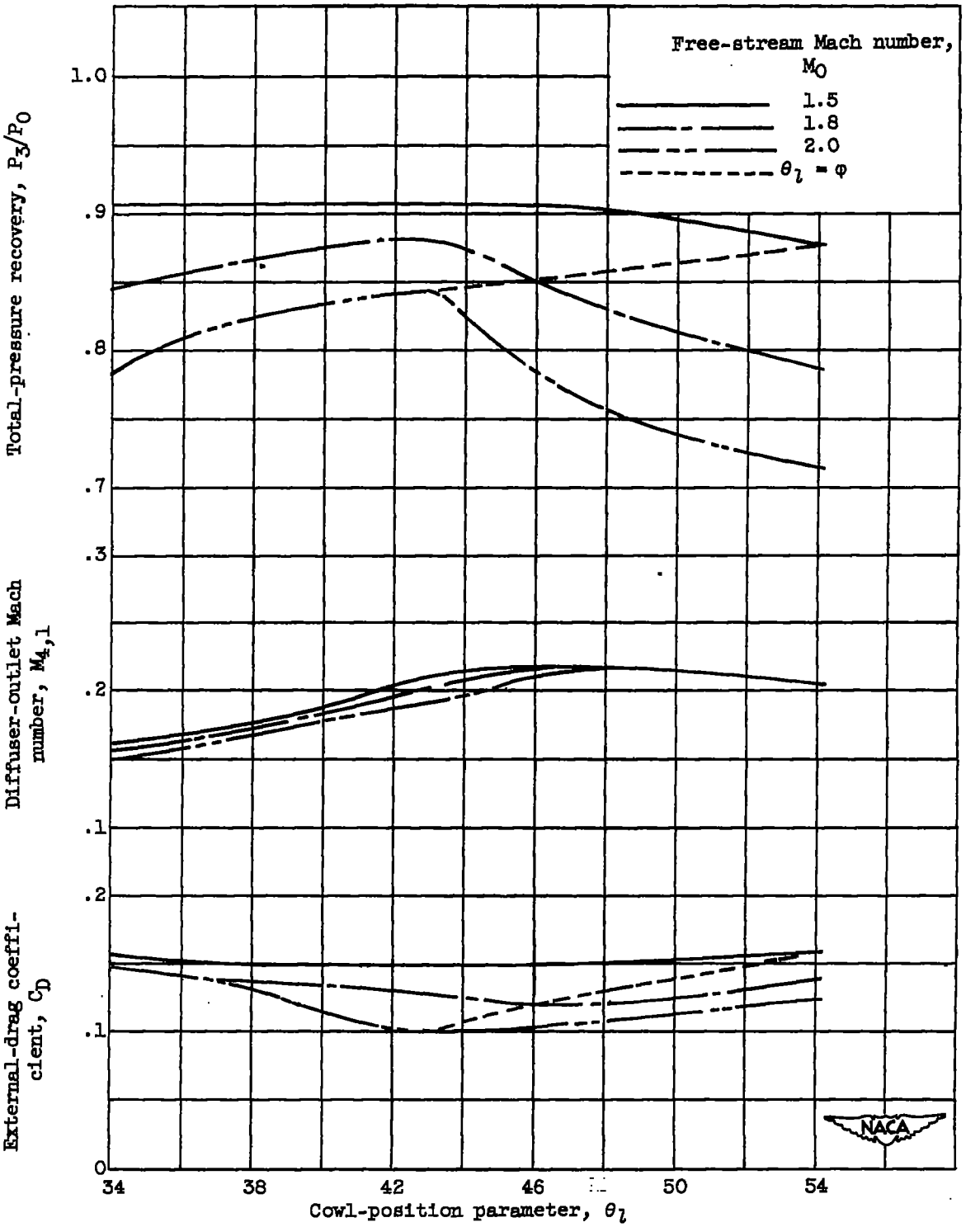

Figure 4. - Effect of spike translation on inlet characteristics at critical operation for zero angle of attack.

2948

CC-3 back

(a) M_0, 2.0; θ_l, 43.0. (b) M_0, 2.0; θ_l, 39.3. (c) M_0, 2.0; θ_l, 36.5. (d) M_0, 2.0; θ_l, 34.1.

(e) M_0, 1.8; θ_l, 45.8. (f) M_0, 1.8; θ_l, 39.3. (g) M_0, 1.8; θ_l, 36.5. (h) M_0, 1.8; θ_l, 34.1.

(i) M_0, 1.5; θ_l, 54.1. (j) M_0, 1.5; θ_l, 39.3. (k) M_0, 1.5; θ_l, 36.5. (l) M_0, 1.5; θ_l, 34.1.

C-33181

Figure 5. - Schlieren photographs of translating-spike inlet at various values of free-stream Mach number M_0 and cowl-position parameter θ_l at zero angle of attack.

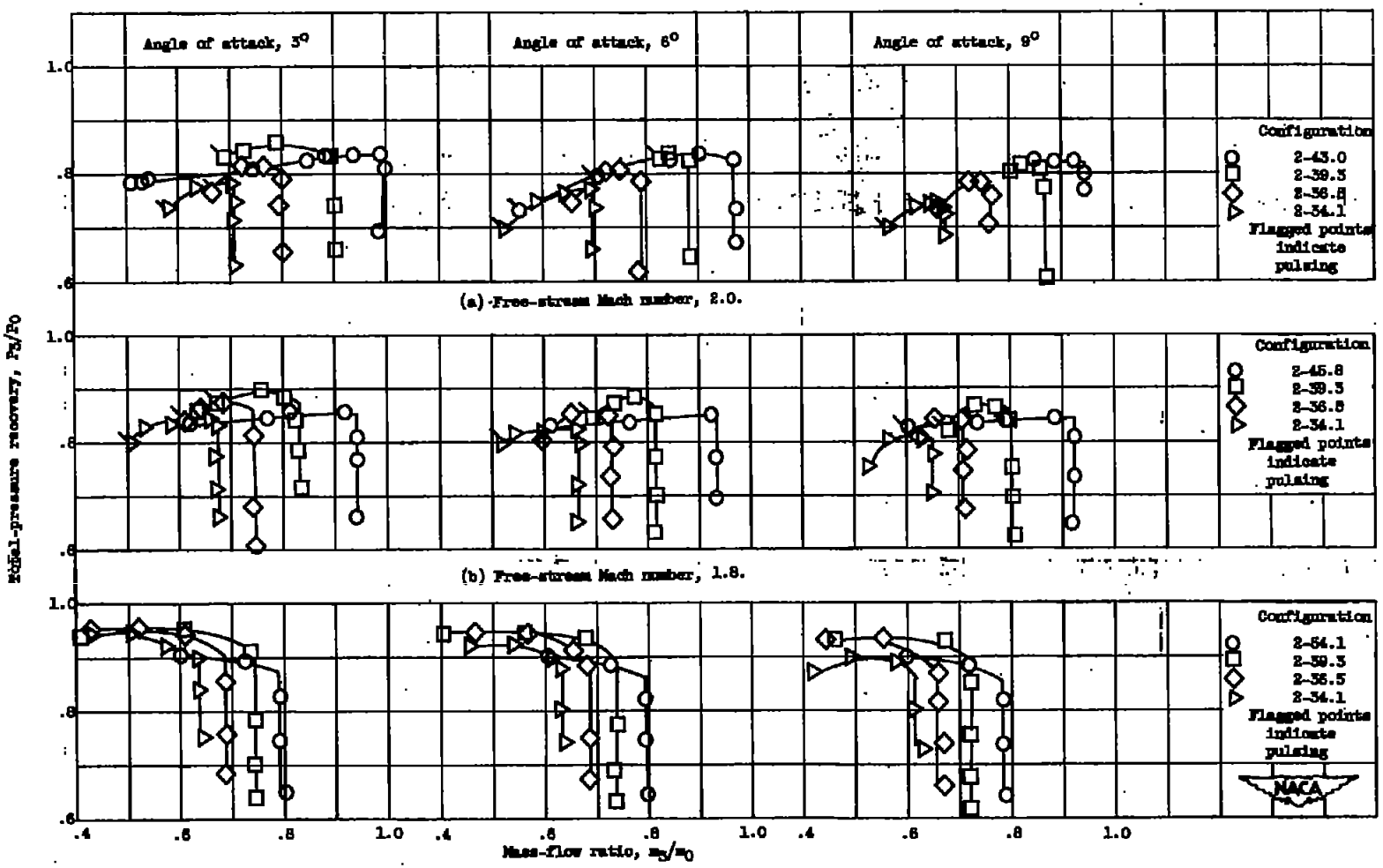

(a) Free-stream Mach number, 2.0.

(b) Free-stream Mach number, 1.8.

(c) Free-stream Mach number, 1.5.

Figure 6. - Total-pressure recovery characteristics at angle of attack for various configurations.

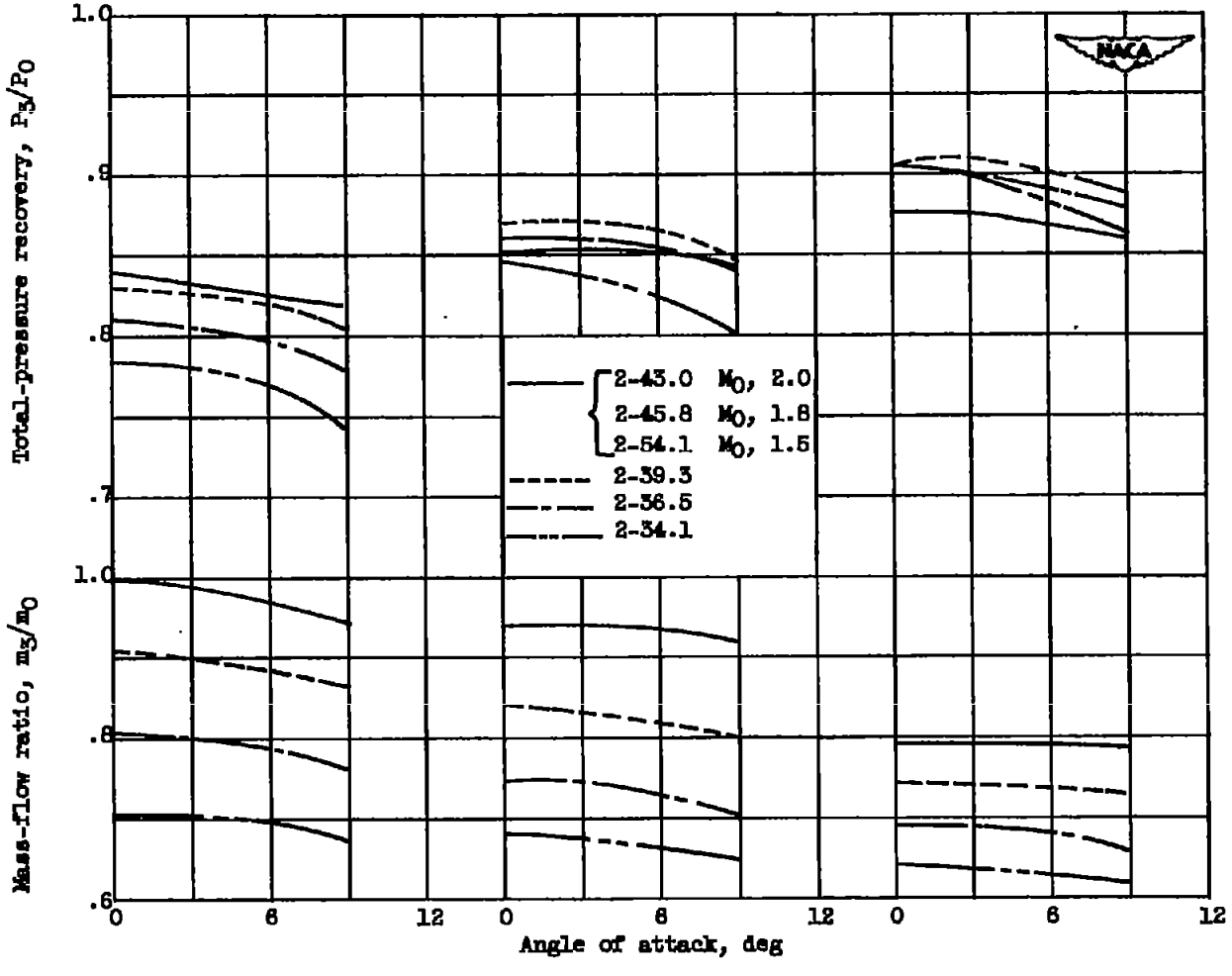

(a) Free-stream Mach number, 2.0.

(b) Free-stream Mach number, 1.8.

(c) Free-stream Mach number, 1.5.

Figure 7. - Effect of angle of attack on translating-spike inlet at critical operation.

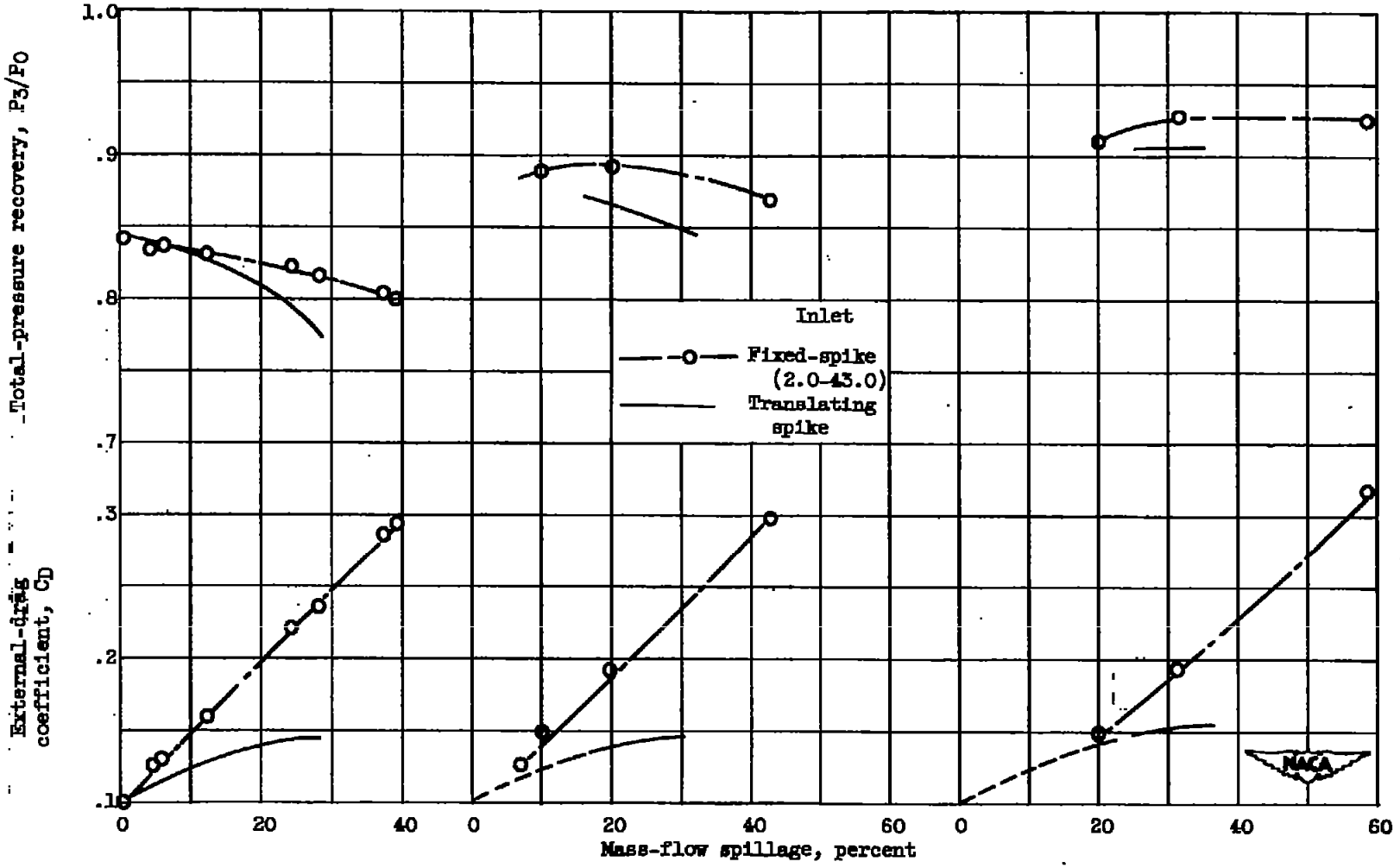

(a) Free-stream Mach number, 2.0.

(b) Free-stream Mach number, 1.8.

(c) Free-stream Mach number, 1.5.

Figure 8. - Comparison of translating-spike inlet characteristics at critical operation with subcritical operation of fixed-spike inlet at zero angle of attack.

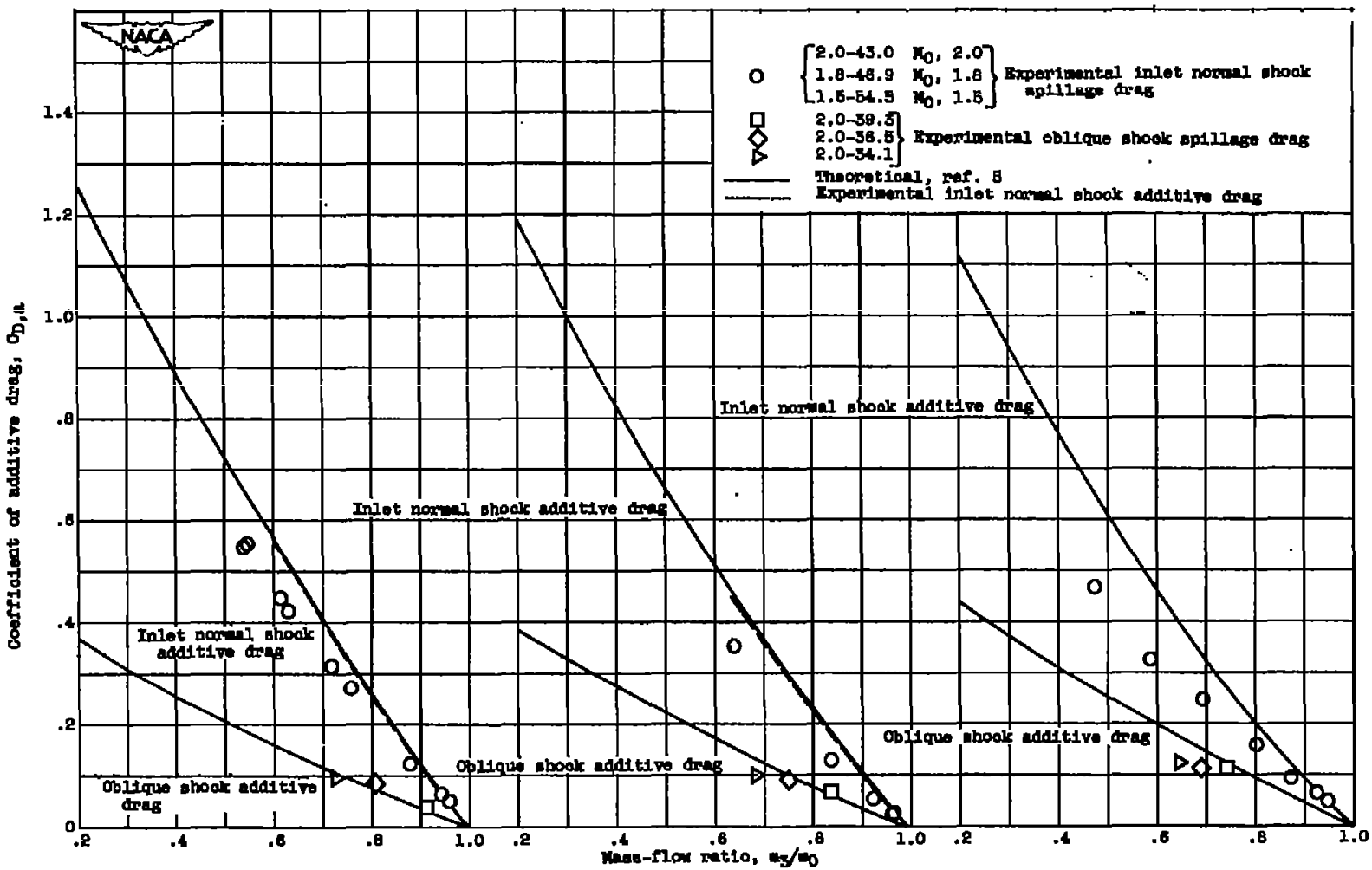

(a) Free-stream Mach number, 2.0. (b) Free-stream Mach number, 1.8. (c) Free-stream Mach number, 1.5.

Figure 9. - Comparison of theoretical and experimental values of additive drag for annular 50° conical inlet.

NACA-Langley - 10-20-53 - 325